GEO Spacecraft Worst-Case Charging Estimation by Numerical Simulation

J.C. Matéo-Vélez, C. Pignal, N. Balcon, D. Payan, P. Sarrailh, S.L.G. Hess

(Abstract No 147)

GEO Spacecraft Worst-Case Charging Estimation by Numerical Simulation

J.-C. Matéo-Vélez, C. Pignal, N. Balcon, D. Payan, P. Sarrailh, S. Hess

***Abstract*— This paper presents a numerical estimation of spacecraft surface charging that combines the effects of both spacecraft material properties and severe environments, often called worst-cases. A series of simulations with the SPIS-GEO tool (Spacecraft Plasma Interaction Software) is analysed in order to determine if a worst-case environment can be extracted from the literature. The simulation especially focuses on the conductivity parameters, especially radiation induced. It is found hardly feasible to define a single and global worst-case, applicable to all situations.**

***Keywords*— spacecraft charging, worst-case environment, radiation induced conductivity**

I. Introduction

Spacecraft charging under geostationary orbit (GEO) can reach thousands of volts negative when submitted to geomagnetic sub-storms. A direct consequence of such events is the generation of large differential potentials on the spacecraft surface, and possibly deteriorations due to electrostatic discharges (ESD). Space industry generally adopts two approaches to assess spacecraft safety. First, ground testing permits to estimate the charging levels leading to ESD on specific and sensitive elements, such as solar cells or cables. This helps avoiding dangerous configurations, such as secondary arcing fed by the spacecraft power itself. This latter mechanism was indeed identified as the most probable cause of ADEOS-II loss in 2002 ([1]-[2]). The second approach consists in estimating charging levels probability by means of numerical simulation ([3]-[7]). This kind of simulation relies on strong assumptions since spacecraft charging is a complex interaction between an ambient radiative environment (electron, proton, photon), the spacecraft geometry and of course materials on its surface. This approach does need measurements of: 1/ ambient environments, especially during strong events, and 2/ material properties. A companion paper provides environments extracted from LANL data and a set of worst-case electron spectra [8]. These environments add to worst-case environments used world-wide and listed in [9]. Material properties such as radiation induced conductivity impacts surface differential charging. This latter property is shown to depend a lot on dose, dose rate, temperature and electric field in companion papers ([10]-[11]).

The objective of this paper is to estimate if a classification of worst-case environment for GEO surface charging is a reachable task. The aim of such a work would consist in obtaining a single worst-case definition, applicable to all GEO missions. This is far from being evident since spacecraft configurations vary a lot, especially material properties. In this paper, we intend to demonstrate that defining a worst-case depends on the criterion chosen to define a dangerous situation. We aim also at showing that the integrated electron flux is not the only relevant parameter, since medium electron energy can modify material properties. The role of low energy protons is also identified in some cases.

Section II describes the simulated spacecraft configuration. In Section III, we compare spacecraft charging results obtained for the worst-case spectra listed in [9]. Material bulk conductivity and radiation induced conductivity are tested in section IV and V respectively. While previous sections concentrate on inverted voltage gradient situation of sunlit dielectrics, Section VI presents results for shaded dielectrics, in the normal gradient situation. Finally, Section VII presents the main outcomes of this study.

II. Simulation Description

All simulations are performed with the SPIS tool version 5.1 [4], already used to simulate various GEO spacecraft charging situations ([3], [14]). The spacecraft geometry is described in Fig. 2 and Fig. 3. It is composed of a spacecraft hub of dimensions 1.76*2.64*2.64 m, two circular antennas of diameter 2.00 m and thickness 0.15 m, a cylindrical antenna of diameter 1.00 m and length 0.88 m and finally two solar arrays of dimensions 7.04*4.40*0.15 m. The list of materials properties is given in Fig. 1.

The differential energy distributions of the environments used in this work are given in Fig. 4 and graphically compared in Fig. 5. They were extracted from [9]. In this plot, environments with a single (*) denote single maxwellian environments, while (**) denotes double maxwellian. Note that the ECSS-E-ST-10-04C and SCATHA-Mullen double maxwellian have been used as they are, and also used with a removal of the low energy populations.

J.-C. Matéo-Vélez, C. Pignal, P. Sarrailh and S. Hess are with ONERA - The French Aerospace Lab, Toulouse, France (e-mail: Mateo@onera.fr)
N. Balcon and D. Payan are with CNES (e-mail: Denis.Payan@cnes.fr).

(Abstract No 147)

SPIS	TE2K	OSR2K	BK2K	NP2K	GR2K	SC2K	CFRP	KAPTON (RF 1/21600 DESP)
RDC	2	4,8	3,5	3,5	3,5	3,8	1	3,46
DMT	1,27E-04	1,50E-04	2,50E-06	5,00E-05	1,27E-04	1,25E-04	1,00E-03	2,50E-05
BUC	1,00E-16	1,00E-17	-1	5,90E-14	-1	1,00E-17	-1	1,00E-19
ATN	7	10	5	5	6	10	6,34	5
M SEY	3	3,3	2,1	2,1	1	5,8	0,7	1,46
PEE	0,3	0,5	0,15	0,15	0,3	1	0,3	0,245
RPR1	45,4	116,3	71,48	-1	-1	77,5	110	70
RPN1	0,4	0,81	0,6	0	0	0,45	1,9	0,6
RPR2	218	183,1	312,1	1,05	2	156,1	300	300
RPN2	1,77	1,86	1,77	9,8	12	1,73	1,04	1,75
SEY	0,455	0,455	0,455	0,455	0,455	0,244	0,413	0,455
IPE	140	140	140	140	140	230	135	140
PEY	2,00E-05	2,00E-05	5,00E-06	2,00E-05	7,20E-06	1,20E-05	7,20E-06	5,70E-07
SRE	1,00E+16	1,00E+19	-1	1,00E+13	-1	1,00E+19	-1	1,00E+20
MAP	19	20	12,01	12,01	12,01	20	10000	10000
MPD	2150	2660	1600	1600	1600	2660	11000	2000
RCC	0	0	0	0	0	0	1,00E-13	2,08E-13
RCP	1	1	1	1	1	1	1	8,60E-01
MAD	1000	1000	1000	1000	1000	1000	1000	1,42E+03

Fig. 1. Details of reference materials properties. The signification of SPIS properties names can be found in the software user manual embedded in the SPIS release [4]. Te2k refers to teflon, Osr2k to optical sun reflector, bk2k to black kapton, Np2k to non conducting paint, Gr2k to graphite, Sc2k to solar cell cover glass, CFRP to carbon fiber and kapton to material measured at ONERA.

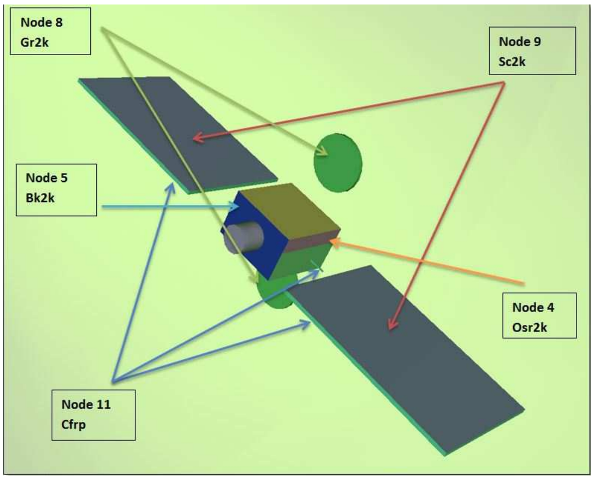

Fig. 2. Spacecraft geometry front side, with covering materials.

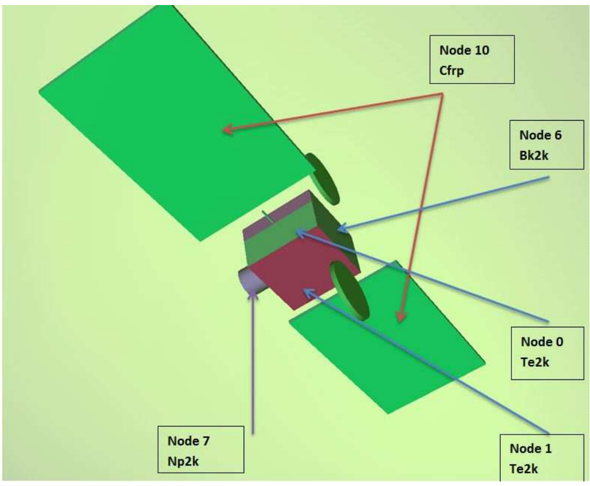

Fig. 3. Spacecraft geometry back side. Nodes 2 and 3 are made of Te2k and are the two non-visible surfaces of the satellite body.

	Ne1 [m-3]	Ni1 [m-3]	Te1 [eV]	Ti1 [eV]	Je1 [A/m2]	Ji1 [A/m2]
10_ECSS**	1,20E+06	1,30E+06	2,75E+04	2,80E+04	5,49E-06	1,40E-07
11_ECSS*	1,20E+06	1,30E+06	2,75E+04	2,80E+04	5,49E-06	1,40E-07
12_NASA*	1,12E+06	2,36E+05	1,20E+04	2,95E+04	3,38E-06	2,61E-08
13_Galaxy15*	4,58E+04	1,00E+05	5,56E+04	7,50E+04	2,98E-07	1,76E-08
14_ATS6*	1,20E+06	2,36E+05	1,60E+04	2,95E+04	4,19E-06	2,61E-08
15_SCATHA1*	2,50E+06	2,90E+06	2,28E+04	1,28E+04	1,04E-05	2,11E-07
16_SCATHA2*	2,50E+06	2,80E+06	1,66E+04	1,16E+04	8,89E-06	1,94E-07
17_SCATHA1**	2,30E+06	1,30E+06	2,48E+04	2,82E+04	9,99E-06	1,41E-07
18_SCATHA1979*	1,40E+06	1,90E+06	2,36E+04	1,93E+04	5,93E-06	1,70E-07
	Ne2 [m-3]	Ni2 [m-3]	Te2 [eV]	Ti2 [eV]	Je2 [A/m2]	Ji2 [A/m2]
10_ECSS**	2,00E+05	6,00E+05	4,00E+02	2,00E+02	1,10E-07	5,46E-09
11_ECSS*						
12_NASA*						
13_Galaxy15*						
14_ATS6*						
15_SCATHA1*						
16_SCATHA2*						
17_SCATHA1**	2,00E+05	1,60E+06	4,00E+02	3,00E+02	1,10E-07	1,78E-08
18_SCATHA1979*						

Fig. 4. Published worst-case environments characteristics. All are maxwellian energy distributions.

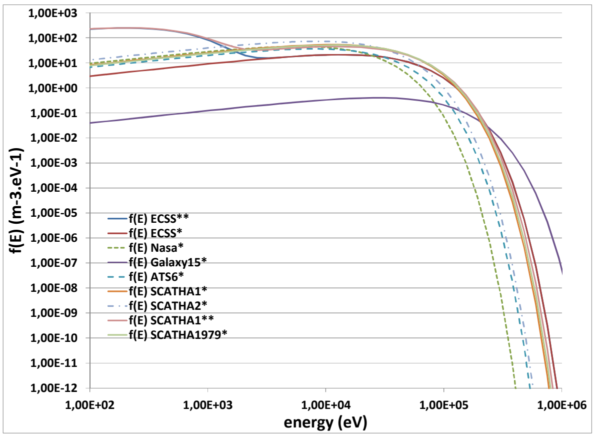

Fig. 5. Differential energy distribution of published worst-cases

Spacecraft charging risks are studied following two criteria: 1/ Time to reach 500 V of inverted voltage gradient between the solar cells and the spacecraft ground, which is known to be a sensitive situation; 2/ Gradient obtained at the same place but at a time close to equilibrium (200s and 1000s pending on the cases).

III. Published Worst-Cases Environments Comparison

This section presents the comparison of results obtained with the reference spacecraft configuration of Part II. We focus first on eclipse condition, and then on a spacecraft at Sun.

A. *Eclipse Condition*

The results of simulations made in eclipse condition are presented in Fig. 6, which shows the absolute ground spacecraft potential. Charging dynamics varies from an environment to another, pending on their integrated fluxes. Large fluxes lead to a quick charging phase. Some environments (Scatha2*, Nasa* and ATS-6) lead to a slower

(Abstract No 147)

initial decrease because electron collection is mitigated by a larger secondary electron emission at energies around 15 keV (instead of 25 keV for other environments), see Fig. 9. The Galaxy-15 environment leads to a slow evolution because the electron density and current density are small, even though the temperature is large. These initial transient phases are followed by a slow decrease of the absolute potential, which is ruled by differential charging. During this phase, the spacecraft structure gets more negative while the solar cell cover glasses gets less negative due to their strong secondary electron emission yield under electron impact (property MSEY), see Fig. 7. The capacitive coupling is ruled by thin dielectric layer, hence with a slow dynamics *wrt* to initial absolute spacecraft capacitance.

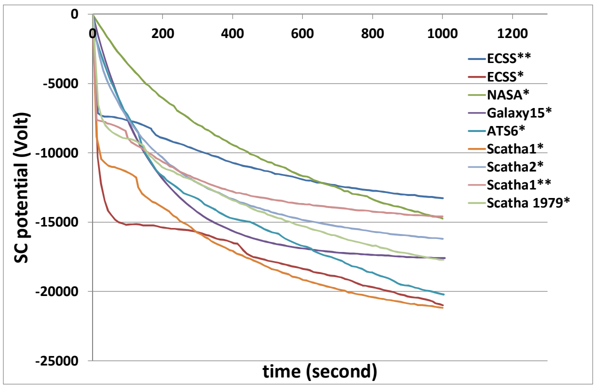

Fig. 6. Spacecraft potential versus time in Eclipse condition

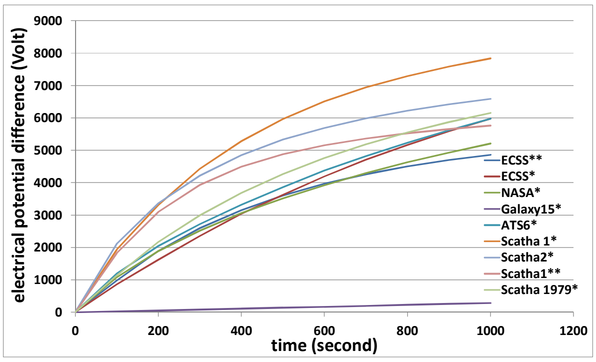

Fig. 7. Electrical potential difference between solar cells and SC versus time in eclipse condition

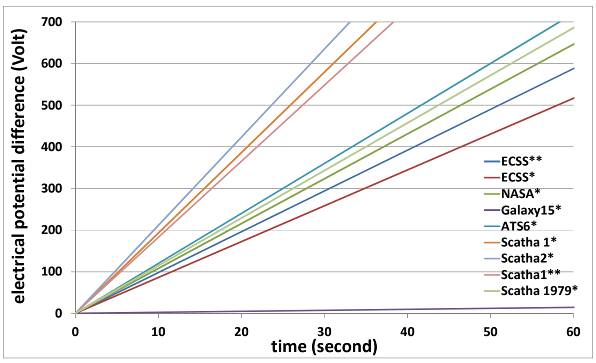

Fig. 8. Zoom of solar cells cover glasses potential difference in eclipse condition. The value of 500 V is of specific interest.

The ECSS* case evolves quickly to a large negative potential (- 21 000V) while the NASA* case leads slightly to a significantly less negative potential (-13 000V). This is a combination of electron current flux, which tends to make the spacecraft float negative, and secondary electron emission under electron impact (SEEE) and proton impact (SEEP), which tend to mitigate that potential. For SEEE, the more important the integrated surface of the differential energy distribution will be between the two cross-over energies, the less important the absolute potential of the spacecraft will be (absolute value). As a result, different spectra lead to different secondary emission yields. Differential charging is qualitatively the same for all spectra except the Galaxy15 case which does not exhibits any significant charging, see Fig. 7. This is due to the very large electron temperature of more than 50 keV. SEEE yield is small at those energies for all materials, as shown in Fig. 9, and the net currents are thus almost homogeneous over the spacecraft.

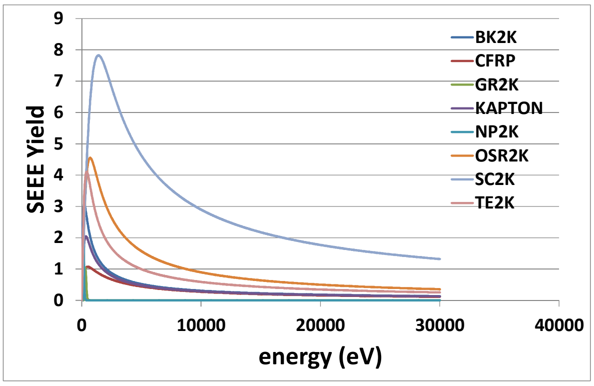

Fig. 9. SEEE yield versus electron impact energy for different materials, considering an isotropic electron flux

Eclipse			
Criterion 500V	time	Criterion t=1000s	epd
Scatha2*	18s	Scatha1*	7838V
Scatha1*	24s	Scatha2*	6585V
Scatha1**	26s	Scatha1979*	6156V
ATS6*	37s	ATS6*	5978V
Scatha1979*	39s	ECSS*	5977V
NASA*	42s	Scatha1**	5762V
ECSS**	49s	NASA*	5208V
ECSS*	57s	ECSS**	4863V
Galaxy15*	> 1000s	Galaxy15*	288V

Fig. 10. Environment classifications in eclipse condition

The environment classification of Fig. 10 shows that Scatha-Mullen 1 and 2 are the most risky when looking at the first criterion. The second criterion is less evident since environments that are initially less risky tend to get more

(Abstract No 147)

dangerous than others after a while. We explain this in Part III-C.

Fig. 11 and Fig. 12 present the spacecraft surface potential in the Scatha1* environment. Solar cells are in the inverted potential gradient situation, as said earlier, while other dielectrics are generally more negative than the spacecraft potential of -21000 V.

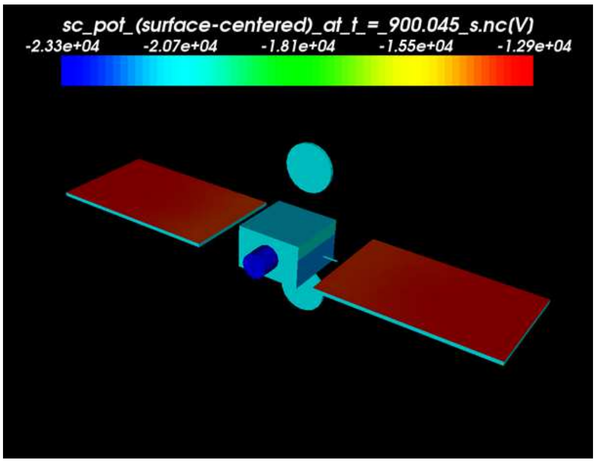

Fig. 11. Surface potentials on the front side of the spacecraft (eclipse condition, Scatha1* case)

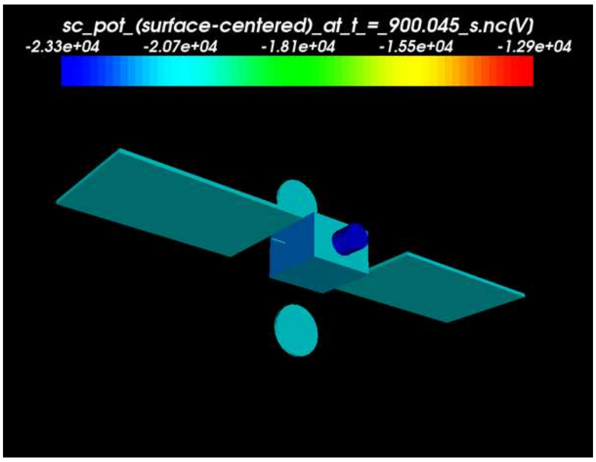

Fig. 12. Surface potentials on the back side of the spacecraft (Eclipse condition, Scatha1* case)

B. Sunlight Condition

This part gathers the results for a sunlight illumination perpendicularly to the solar arrays, see Fig. 13 and Fig. 14. Differential potentials of all surfaces are plotted in Fig. 15 and Fig. 16. The sunlit dielectrics are significantly less negative than the spacecraft ground. Shaded faces are much more negative than previously in eclipse. This is due to the fact that photoemission tends to keep the spacecraft ground less negative while the shaded dielectrics still keep getting more and more negative (if we forget conductivity...).

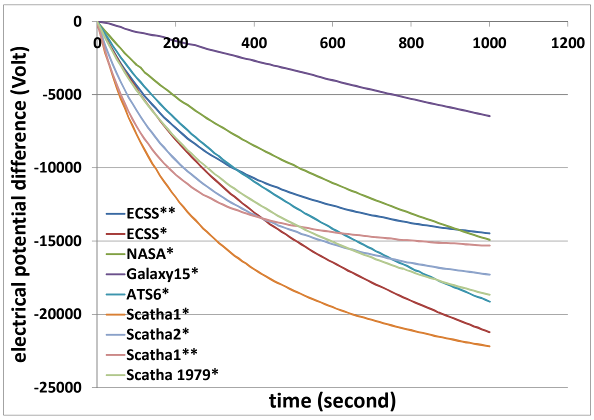

Fig. 13. Spacecraft potential versus time in Sunlight condition

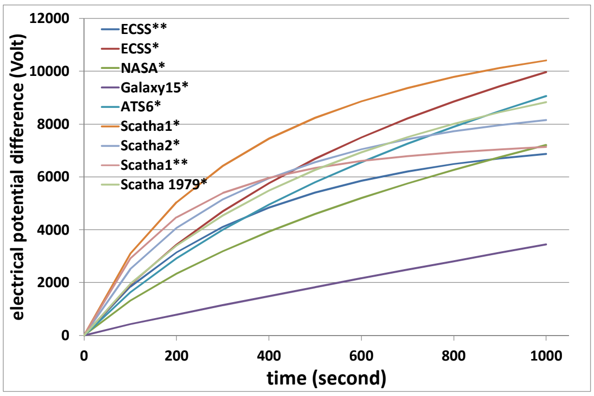

Fig. 14. Electrical potential difference between solar cells and SC versus time in Sunlight condition

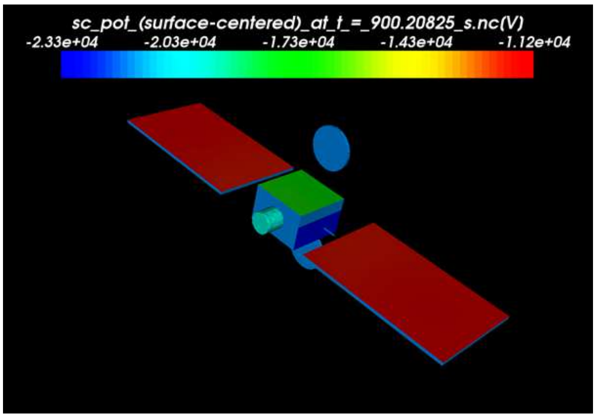

Fig. 15. Surface potentials on SC in sunlight condition (front side)

(Abstract No 147)

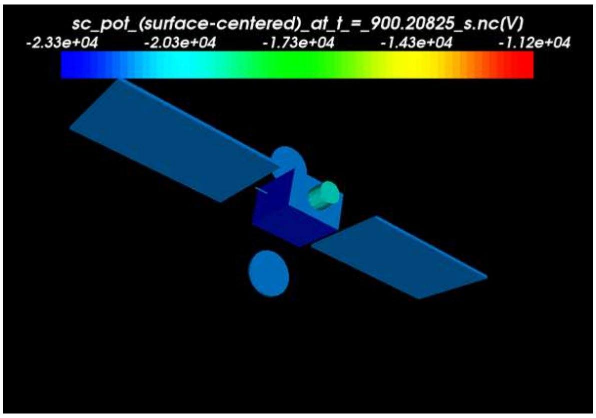

Fig. 16. Surface potentials on SC in sunlight condition (back side)

Sun			
Criterion 500V	time	Criterion t=1000s	epd
Scatha1*	13s	Scatha1*	10409V
Scatha1**	13s	ECSS*	9965V
Scatha2*	15s	ATS6*	9059V
Scatha1979*	22s	Scatha1979*	8832V
ECSS*	23s	Scatha2*	8150V
ECSS**	24s	NASA*	7205V
ATS6*	27s	Scatha1**	7139V
NASA*	35s	ECSS**	6872V
Galaxy15*	120s	Galaxy15*	3441V

Fig. 17. Environment classifications in sunlight condition

The environment classification of Fig. 17 concludes that Scatha1* case is the worst-case in sunlight for this spacecraft configuration, and following the two criteria. However, the rest of the classification changes when looking the second criterion. This is explained in the next part.

C. *Low energy protons effect*

As seen in Fig. 13, some curves depart from their initial strong voltage increase after a while, typically 200 s. Theses curves are double maxwellian ECSS and SCATHA1. They can be compared with their respective single maxwellian. Initially, they are ranked at the first positions of the worst-case classification of Fig. 17. After 1000 s, they are the last ones. The effect is almost negligible during the first 100 s, because the high energy electron population contributes equally to spacecraft charging. Low energy electrons have no impact since they are completely repelled by the -1000 V (and more) potentials. After that point, the single Maxwellian departs from the double-Maxwellian results because of low energy protons. Indeed, their flux is greatly enhanced due to focusing and acceleration towards the negative elements of the spacecraft. The Orbit Limited Model (OML) states that the flux is multiplied by a factor $1-q\phi/kT$, where q and kT are the population charge and temperature (in eV) respectively, ϕ the surface potential. For 200 eV protons for instance, the OML factor can reach 100 at ϕ = -20 000V. In addition, protons are accelerated by the strongly attracting potential. Secondary electron emission under proton impact (SEEP) is close to a factor 2 or 4 for protons of energy 20 000 eV, as seen in Fig. 18.

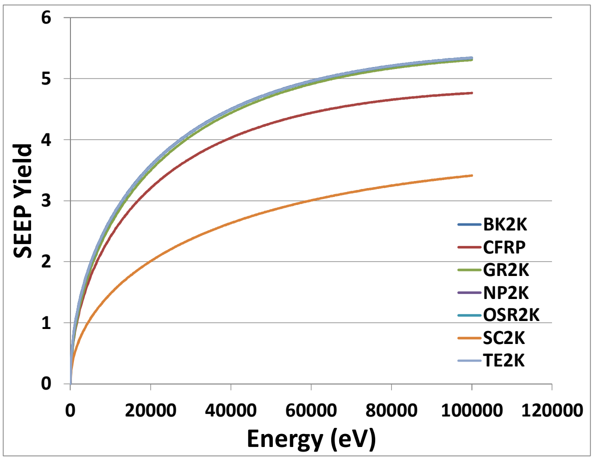

Fig. 18. SEEP yield versus proton impact energy for different materials, and isotropic proton fluxes

The low and high energy proton fluxes are multiplied by a factor of 200 to 400 and 4 to 8 respectively, which makes both of them comparable to the electron flux. Taking into account low energy populations has a significant effect on long duration and large charging events (thousands of volts, second criterion). The 500 V criterion however does not rely on SEEP, since it appears at smaller voltages (hundreds of volts).

IV. Bulk Conductivity Influence

In this section, we simulate the same spacecraft configuration as in Part III, with the SCATHA-1* environment, except that we modify the bulk conductivity of the solar cells cover glasses. It is known that this material property strongly evolves with temperature from very resistive at -150°C to intermediate values at 20°C and almost conductive at large temperatures 100°C. As a consequence, we have performed a parametric study to take account of cold, medium and hot cover glasses, using bulk conductivities of 1e-17, 1e-13 and 1e-10 $ohm^{-1}.m^{-1}$ respectively. The large conductivity configuration leads to a very small spacecraft absolute charging and cover glass differential charging. The intermediate value divides by a factor two the potentials with respect to cold conditions. This highlights the importance of taking into account temperature effects. This is especially important for eclipse exit in particular, during which cover glasses remain cold during a certain amount of time. At eclipse exit, the spacecraft may be pre-charged.

(Abstract No 147)

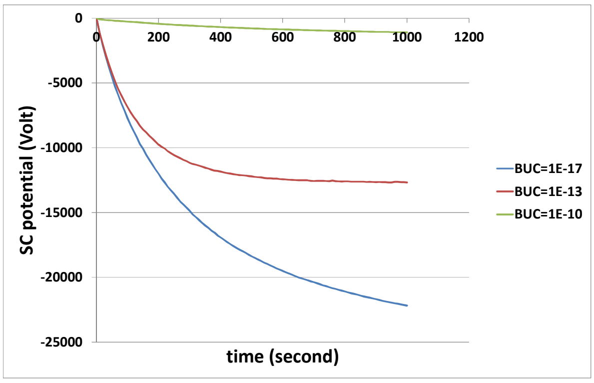

Fig. 19. Spacecraft potential versus time in Sunlight condition with 3 different BUC parameters (Scatha1* case)

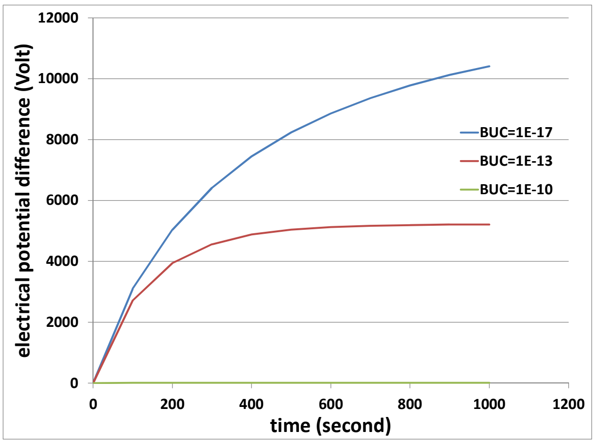

Fig. 20. Electrical potential difference between solar cells and SC versus time in Sunlight condition with 3 different BUC parameters (Scatha1* case)

V. Radiation Induced Conductivity (RIC) influence

A. Illustration of RIC effect

The radiation induced conductivity also strongly influences differential charging and so on absolute charging. In this section, we present results obtained in the same configuration as in Part III except that the radiation induced conductivity is now simulated (material parameter RCC different from zero). The radiation induced conductivity σ_{RIC} writes:

$$\sigma_{RIC} = RCC\left(\frac{dD}{dt}\right)^{RCP}$$

where D is the dose (dD/dt is the dose rate). In this simulation, we varied RCC from 0 to 1e-10 ohm^{-1}.m^{-1} only for cover glass material, while RCP is kept constant to 1. A large RIC induces a small spacecraft potential because it makes cover glasses almost conductive which in turn leads to a significant current leakage from the shaded solar array to the sunlit emitting surfaces. Shaded faces can no longer float very negative and impose a significant negative barrier of potential for photoelectrons emitted by sunlit dielectric. This results in a less negative net current and a less negative spacecraft.

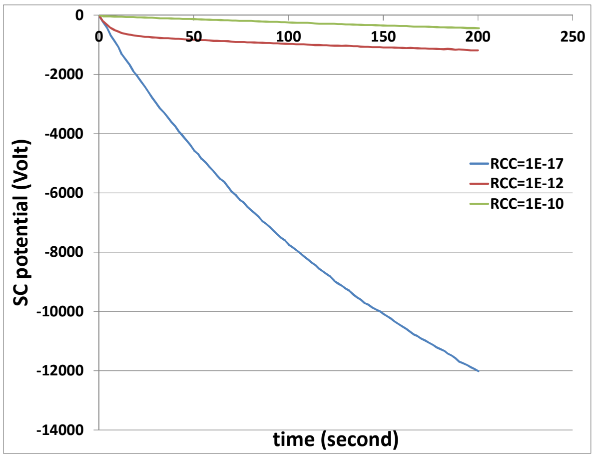

Fig. 21. Spacecraft potential versus time in Sunlight condition with 3 different RCC parameters (Scatha1* case)

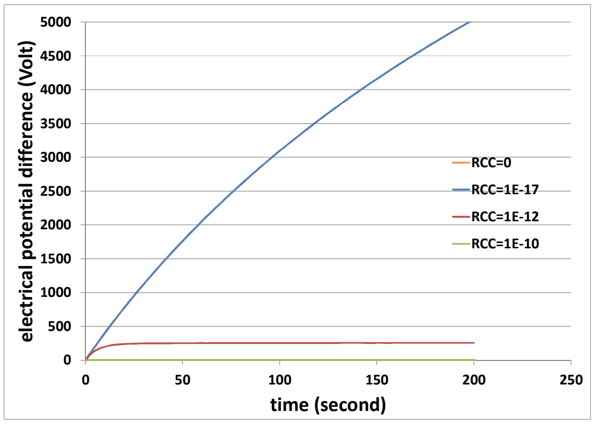

Fig. 22. Electrical potential difference between solar cells and SC versus time in Sunlight condition with 3 different RCC parameters (Scatha1* case)

B. Published worst-cases comparison with intermediate RIC

In this paragraph we simulate all environments with a cover glass RCC parameter of 1e-12 ohm^{-1}.m^{-1} (instead of 0) and RCD = 1. The effect is very significant for all environments except three of them: NASA*, ATS6* and Scatha2*. These environments still lead to potentials above -5000 V, while others generate less than -1000 V after 200 s. This is clearly linked to the presence or absence of medium energy electrons in the environment. The dashed curves of Fig. 5, representing the environments leading to strong charging, show lower energy distribution functions around 100-500 keV. Thus in these three specific cases, less electrons are concerned with high energies and RIC reduced. I this case, the worst-case environment would rather be Scatha2*, ATS6* and NASA*.

(Abstract No 147)

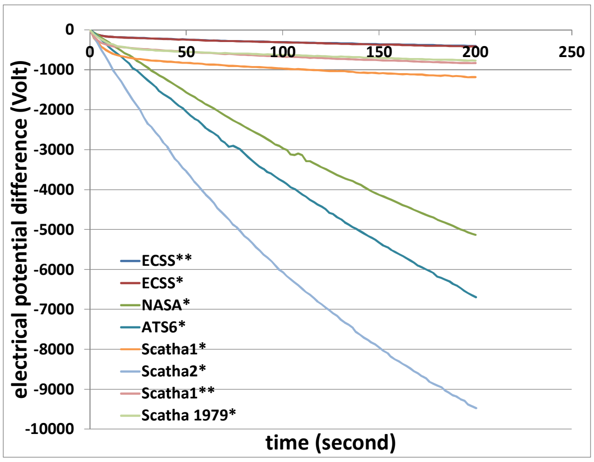

Fig. 23. Spacecraft potential versus time in Sunlight condition with RCC = 1E-12 $ohm^{-1}.m^{-1}$

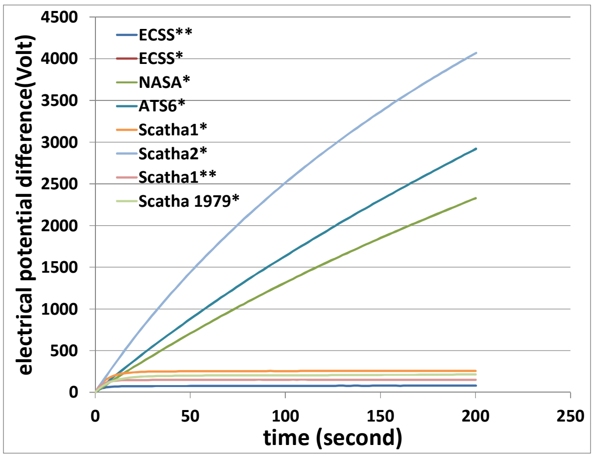

Fig. 24. Electrical potential difference between solar cells SC versus time in Sunlight condition with RCC = 1E-12 $ohm^{-1}.m^{-1}$

Sun RCC12				
Criterion 500V	time	stabilized value	Criterion t=200s	epd
Scatha2*	15s		Scatha2*	4069V
ATS6*	27s		ATS6*	2920V
NASA*	34s		NASA*	2327V
Scatha1*	> 200s	256V	Scatha1*	256V
Scatha1979*	> 200s	213V	Scatha1979*	213V
Scatha1**	> 200s	149V	Scatha1**	149V
ECSS**	> 200s	78V	ECSS**	78V
ECSS*	> 200s	77V	ECSS*	77V
Galaxy15*			Galaxy15*	

Fig. 25. Worst-cases depending on the criterion in Sunlight condition with RCC = 1E-12

VI. Charging of Shaded Dielectrics

In this section, we simulated the same spacecraft configuration as in Part III, except that we modified the back side of solar panels: CFRP was replaced with Kapton® (see material properties in Fig. 1).In order to see the RIC parameter influence, two simulations have been made, the first one with the proper RCC parameter of kapton and the second one with RCC = 0.

Both cases have no influence on the worst-case classification following the two criteria expressed earlier (concerning the differential charging between cover glass and SC). But as seen on Fig. 26 and Fig. 27, the behavior of differential charging between kapton and SC is greatly conditioned by RIC. In the same way as in Part V.B, three cases (Scatha2*, ATS6* and NASA*) are much less affected by RIC because of a smaller flux of high energy electrons. For shaded kapton, NASA* becomes the worst-case environment. The classification is changed because of the narrow link between differential energy distribution and RIC.

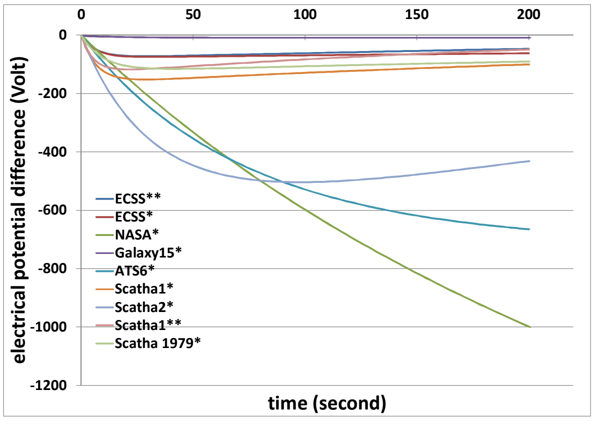

Fig. 26. Electrical potential difference between back side of solar panels and SC versus time in Sunlight condition with back side of solar panels made with kapton

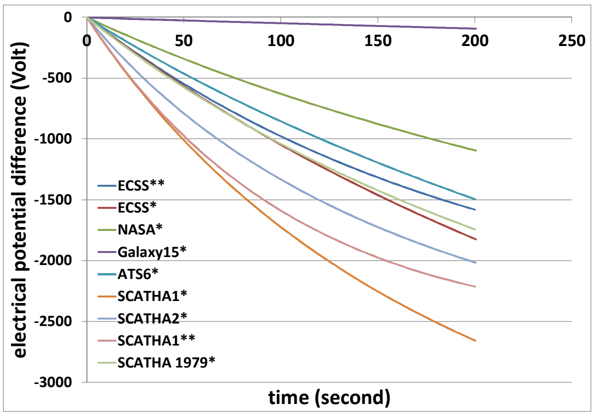

Fig. 27. Electrical potential difference between back side of solar panels (kapton, RCC=0) and SC versus time in sunlight condition

Shaded dielectrics may reach large normal potential gradient situations (NPG), *i.e.* significantly negative *wrt* the spacecraft ground. Thanks to its good RIC properties, kapton is a good candidate to avoid that risk. Other materials could lead to ESD, and their occurrence close to power supply carriers (solar cells, wires, etc) may produce hazardous secondary arcing. To assess that risk, RIC properties are key parameters.

(Abstract No 147)

VII. SUMMARY

In this paper, we have identified different worst-case environments for a single spacecraft configuration pending on the materials used on it, and pending on the criteria used to define them. Bulk and radiation induced conductivities determine the absolute and differential charging situation, as well as secondary electron emission. Cover glasses are known to have negligible radiation induced conductivity. As a consequence, for such materials, the criteria based on the solar cell coverglass differential voltage mainly depend on the integrated electron flux, rather than on their distributions at intermediate energy (producing RIC). More in detail, the worst-case classification changes when looking at either the time to reach a 500 V inverted voltage gradient (about some tens of seconds), or the potentials reached after a large duration (kilovolts after some hundreds of seconds). For this latter case, the presence of a low energy proton flux is of prime importance since it is a good way to limit large negative potentials (above -10 000 V). For both criteria based on solar cell cover glass potential, Scatha1* is the worst-case environment simulated in this paper.

However, the picture is not so clear when considering: 1/ sunlit dielectrics with a significant RIC conductivity; 2/ shaded dielectrics, which may also charge up and trigger hazardous ESDs; 3/ the effect of temperature changes when exiting eclipse for instance. For these important cases, the worst-case environments classification may significantly change from a case to another, pending on the materials used and their localization. In conclusion, it seems hardly feasible to distinguish one worst-case among the others without performing such an analysis, and taking into account conductivity under irradiation.

As a perspective, we plan to perform exhaustive simulations using also the environments taken from [8] that computed LANL spacecrafts data over a period of 15 years. It will deal with electron fluxes with intermediate energy. This activity also highlights the needs to use consolidated conductivity measurements and on-orbit spectra data. Recent data could be used ([10]-[13]).

REFERENCES

[1] M. Nakamura, "Space plasma environment at the ADEOS-II anomaly" in Proc. 9th Spaceraft Charging Technol. Conf, Tsukuba, Japan, Apr 4-8, 2005.

[2] S. Kawakita et al., "investigation of operational anomaly of ADEOS-II satellie", in Proc. 9th Spaceraft Charging Technol. Conf, Tsukuba, Japan, Apr 4-8, 2005.

[3] J.-F. Roussel, G. Dufour, J.-C. Mateo-Velez, B. Thiébault, B. Andersson, D. Rodgers, A. Hilgers, D. Payan, SPIS multi time scale and multi physics capabilities: development and application to GEO charging and flashover modelling, IEEE Trans. Plasma Sci., Vol 40, N°2, 2012

[4] www.spis.org

[5] I. Katz et al., A three dimensional dynamic study of electrostatic charging in materials, NASA-CR-135256, 1977

[6] Validation of NASCAP-2k spacecraft environment interactions calculations, V.A. Davis et al., in Proc 8th SCTC, Huntsville, AL, USA, Oct. 2003.

[7] T. Muranaka et al., "Final version of multi-utility spacecrat charging analysis tool (MUSCAT)", in Proc 10th SCTC, June 2007.

[8] D. Payan et al., " Worst case of Geostationary charging environment spectrum based on LANL flight data", in Proc. 13th Spaceraft Charging Technol. Conf, Pasadena, California, Jun 23-27, 2014.

[9] D. Ferguson, "AFRL Perspective on Spacecraft Charging Potential Estimation in Worst-Case Environments", AFRL release #4996, ISO WG4 workshop, Tokyo, Japan, Jan 2014.

[10] Th. Paulmier et al. "Charging Properties of New Materials", in Proc. 13th Spaceraft Charging Technol. Conf, Pasadena, California, Jun 23-27, 2014.

[11] Th. Paulmier et al., "Radiation Induced Conductivity Of Space Used Polymers Under High Energy Electron Irradiation", in Proc. 13th Spaceraft Charging Technol. Conf, Pasadena, California, Jun 23-27, 2014.

[12] M. Belhaj et al., "Electron Emission Properties of Space Used Dielectric Materials", in Proc. 13th Spaceraft Charging Technol. Conf, Pasadena, California, Jun 23-27, 2014.

[13] M. Belhaj et al., "Xe erosion effect on the electron emission yield of coverglass", in Proc. 13th Spaceraft Charging Technol. Conf, Pasadena, California, Jun 23-27, 2014.

[14] B. Theillaumas et al., " Simulation and analysis of spacecraft charging using SPIS-GEO and NASCAP-GEO ", in Proc. 13th Spaceraft Charging Technol. Conf, Pasadena, California, Jun 23-27, 2014.

ONERA THE FRENCH AEROSPACE LAB return on innovation

cnes CENTRE NATIONAL D'ÉTUDES SPATIALES

GEO Spacecraft Worst-Case Charging Estimation by Numerical Simulation

J.-C. Matéo-Vélez(1), C. Pignal(1), N. Balcon(2), D. Payan(2), P. Sarrailh(1), S. Hess(1)

(1) ONERA, The French Aerospace Lab, Toulouse F-31055, France

(2) CNES, The French Space Agency, 31401, Toulouse Cedex 9, France

Abstract

This paper presents a numerical estimation of spacecraft surface charging that combines the effects of both spacecraft material properties and severe environments, often called worst-cases. A series of simulations with the SPIS-GEO tool (Spacecraft Plasma Interaction Software) is analyzed in order to determine if a worst-case environment can be extracted from the literature. The simulation especially focuses on the conductivity parameters, especially radiation induced. It is found hardly feasible to define a single and global worst-case, applicable to all situations.

Published worst-cases

	Ne1 [m-3]	Ni1 [m-3]	Te1 [eV]	Ti1 [eV]	Je1 [A/m2]	Ji1 [A/m2]
10_ECSS**	1,20E+06	1,30E+06	2,75E+04	2,80E+04	5,49E-06	1,40E-07
11_ECSS*	1,20E+06	1,30E+06	2,75E+04	2,80E+04	5,49E-06	1,40E-07
12_NASA*	1,12E+06	2,36E+05	1,20E+04	2,95E+04	3,38E-06	2,61E-08
13_Galaxy15*	4,58E+04	1,00E+05	5,56E+04	7,50E+04	2,98E-07	1,76E-08
14_ATS6*	1,20E+06	2,36E+05	1,60E+04	2,95E+04	4,19E-06	2,61E-08
15_SCATHA1*	2,50E+06	2,90E+06	2,28E+04	1,28E+04	1,04E-05	2,11E-07
16_SCATHA2*	2,50E+06	2,80E+06	1,66E+04	1,16E+04	8,89E-06	1,94E-07
17_SCATHA1**	2,30E+06	1,30E+06	2,48E+04	2,82E+04	9,99E-06	1,41E-07
18_SCATHA1979*	1,40E+06	1,90E+06	2,36E+04	1,93E+04	5,93E-06	1,70E-07
	Ne2 [m-3]	Ni2 [m-3]	Te2 [eV]	Ti2 [eV]	Je2 [A/m2]	Ji2 [A/m2]
10_ECSS**	2,00E+05	6,00E+05	4,00E+02	2,00E+02	1,10E-07	5,46E-09
11_ECSS*						
12_NASA*						
13_Galaxy15*						
14_ATS6*						
15_SCATHA1*						
16_SCATHA2*						
17_SCATHA1**	2,00E+05	1,60E+06	4,00E+02	3,00E+02	1,10E-07	1,78E-08
18_SCATHA1979*						

Mono(*) and Bi-Maxwellian(**) environments from flight data

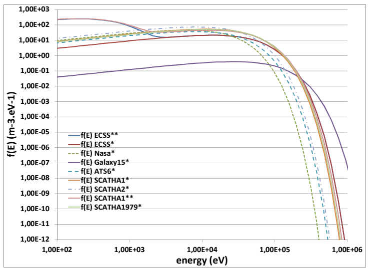

See also paper #143
New data from 15 years of LANL,
D. Payan et al.
"Worst case of Geostationary charging environment spectrum based on LANL flight data"

SPIS Simulations = Parametric Study

SPIS 5.1 used to simulate
- ❑ GEO spacecraft geometry
- ❑ Material properties including
  - ❖ Secondary electron emission under electron (SEEE), proton (SEEP) and photon impact
  - ❖ Conductivity (bulk, surface and radiation induced RIC)
  - ❖ Parametric study : Find a worst-case ?

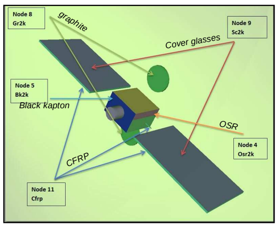

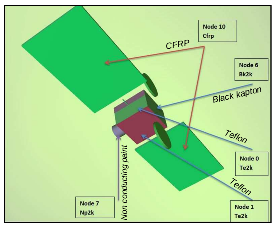

Reference case

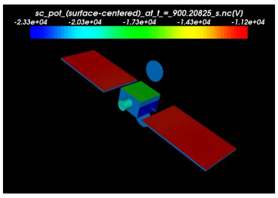

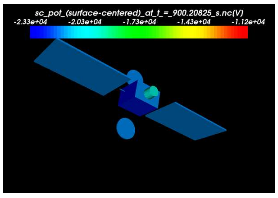

Sun			
Criterion 500V	time	Criterion t=1000s	epd
Scatha1*	13s	Scatha1*	10409V
Scatha1**	13s	ECSS*	9965V
Scatha2*	15s	ATS6*	9059V
Scatha1979*	22s	Scatha1979*	8832V
ECSS*	23s	Scatha2*	8150V
ECSS**	24s	NASA*	7205V
ATS6*	27s	Scatha1**	7139V
NASA*	35s	ECSS**	6872V
Galaxy15*	120s	Galaxy15*	3441V

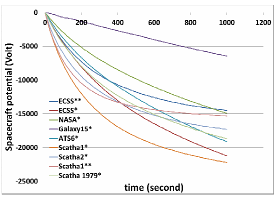

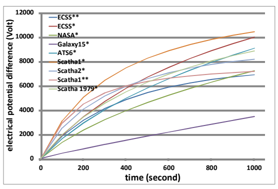

Negative spacecraft charging and Inverted voltage gradient situation for cover glasses

Low energy protons

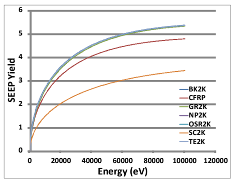

- ❑ No effect at start (see ECSS * and **)
- ❑ Major effect when spacecraft is very negative
  - ❖ OML current increase 1-eϕ/kT
  - ❖ large SEEP yield at large energy

Bulk conductivity of Cover glasses

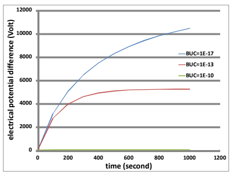

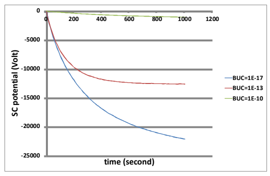

Hot/Cold cover glasses will significantly change absolute and differential charging

Radiation Induced Conductivity of Cover glasses

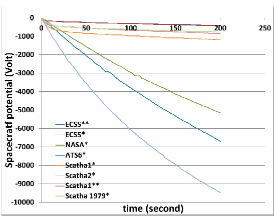

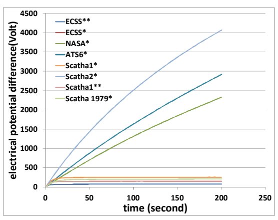

$$\sigma_{RIC} = RCC\left(\frac{dD}{dt}\right)^{RCP}$$

RCC = 1e-12 ohm^{-1}.m^{-1}
RCD = 1

High energy electron flux limits IVG levels

Modifies the worst-case classification

Shaded kapton with and without RIC

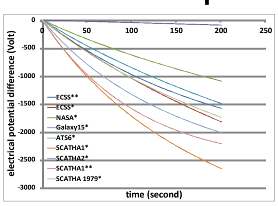

Without RIC: severe charging

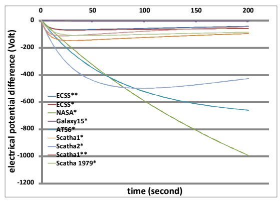

With RIC: limited charging

Conclusion

We have identified different worst-case environments for a single spacecraft configuration pending on the materials used on it, and pending on the criteria used to define them. Bulk and radiation induced conductivities determine the absolute and differential charging situation, as well as secondary electron emission. In addition, shaded dielectrics may also charge up. Finally, the effect of the temperature needs to be investigated. As a perspective, we plan to use taken from paper #143 of LANL spacecrafts data computed over a period of 15 years. It will deal with electron fluxes with intermediate energy. This activity also highlights the needs to use consolidated conductivity measurements and on-orbit spectra data.